Journal of Neurochemistry

JOURNAL OF NEUROCHEMISTRY | 2015 | 133 | 253–265 doi: 10.1111/jnc.13035

ORIGINAL ARTICLE

A novel role for central ACBP/DBI as a regulator of long-chain fatty acid metabolism in astrocytes

Khalil Bouyakdan,*,†,[1] Bouchra Taïb,*,‡,[1] Lionel Budry,*,§ Shangang Zhao,*,† Demetra Rodaros,* Ditte Neess,¶ Susanne Mandrup,¶ Nils. J. Faergeman¶ and Thierry Alquier*,†,‡,§,¶

*Montreal Diabetes Research Center, Centre de Recherche du Centre Hospitalier de l'Universite de Montreal (CRCHUM), Montreal, Quebec, Canada

†Department of Biochemistry, University of Montreal, Montreal, Quebec, Canada

‡Department of Pathology and Cell Biology, University of Montreal, Montreal, Quebec, Canada

§Department of Medicine, University of Montreal, Montreal, Quebec, Canada

¶Villum Center for Bioanalytical Sciences, Department of Biochemistry and Molecular Biology, Southern Denmark University, Odense M, Denmark

Abstract

Acyl-CoA-binding protein (ACBP) is a ubiquitously expressed protein that binds intracellular acyl-CoA esters. Several studies have suggested that ACBP acts as an acyl-CoA pool former and regulates long-chain fatty acids (LCFA) metabolism in peripheral tissues. In the brain, ACBP is known as Diazepam-Binding Inhibitor, a secreted peptide acting as an allosteric modulator of the $GABA_A$ receptor. However, its role in central LCFA metabolism remains unknown. In the present study, we investigated ACBP cellular expression, ACBP regulation of LCFA intracellular metabolism, FA profile, and FA metabolism-related gene expression using ACBP-deficient and control mice. ACBP was mainly found in astrocytes with high expression levels in the mediobasal hypothalamus. We demonstrate that ACBP deficiency alters the central LCFA-CoA profile and impairs unsaturated (oleate, linolenate) but not saturated (palmitate, stearate) LCFA metabolic fluxes in hypothalamic slices and astrocyte cultures. In addition, lack of ACBP differently affects the expression of genes involved in FA metabolism in cortical versus hypothalamic astrocytes. Finally, ACBP deficiency increases FA content and impairs their release in response to palmitate in hypothalamic astrocytes. Collectively, these findings reveal for the first time that central ACBP acts as a regulator of LCFA intracellular metabolism in astrocytes.

Keywords: acyl-CoA, astrocytes, endozepines, fatty acid esterification, fatty acid oxidation, hypothalamus.

J. Neurochem. (2015) **133**, 253–265.

The neural regulation of energy homeostasis mainly relies on the hypothalamus and its capacity to detect circulating nutritional signals such as glucose and long-chain fatty acids (LCFA) (Morton *et al.* 2006). Hypothalamic action of LCFA to modulate glucose homeostasis and food intake is dependent on LCFA esterification in LCFA-CoA but the metabolic

Received June 30, 2014; revised manuscript received December 15, 2014; accepted January 8, 2015.

Address correspondence and reprint requests to Thierry Alquier, CRCHUM-Tour Viger, 900 Saint-Denis, Montreal, QC, Canada, H2X0A9. E-mail: thierry.alquier@umontreal.ca

[1]These authors contributed equally to this work.

Abbreviations used: ACBP, acyl-CoA binding protein; ACC, acetyl-CoA carboxylase; AGPAT, acylglycerol-phosphate acyltransferase; CD36, cluster of differentiation 36; CERS, ceramide synthase; CPT, carnitine palmitoyl transferase; DAG, diacylglycerol; DBI, diazepam-binding inhibitor; DGAT, diacylglycerol acyltransferase; FABP, fatty acid-binding protein; FA, fatty acids; FAS, fatty acid synthase; FATP, fatty acid transport protein; GFAP, glial fibrillary acidic protein; GPAT, glycerol-3-phosphate acyltransferase; Het, heterozygous knockout; KO, homozygous knockout; LCFA, long-chain fatty acids; MBH, mediobasal hypothalamus; MCFA, medium-chain fatty acids; NEFA, non-esterified fatty acid; NeuN, neuronal nuclei; ODN, octadecaneuropeptide; PL, phospholipids; PUFA, polyunsaturated fatty acids; SCD1, stearoyl-CoA desaturase 1; SPTLC, serine palmitoyltransferase long-chain; TAG, triacylglycerol; VLCFA, very long-chain fatty acids; WT, wild-type.

pathways and cell type(s) involved remain elusive (Lam *et al.* 2009).

Once transported into the cell, LCFA are esterified in LCFA-CoA and bound to acyl-CoA-binding protein (ACBP), a highly conserved 10 kDa protein (Burton *et al.* 2005). ACBP is ubiquitously expressed, with high expression levels in tissues with an active lipid metabolism such as the liver and adipose tissues (Faergeman *et al.* 2007), and has a high affinity and specificity for medium to LCFA-CoAs (Rosendal *et al.* 1993). In agreement with its biochemical properties, ACBP deficiency decreases the intracellular LCFA-CoA pool while ACBP over-expression has the opposite effect in yeast (Knudsen *et al.* 1994) and mouse (Huang *et al.* 2005). In addition, gain- and loss-of-function studies have shown that ACBP is required for LCFA esterification into triglycerides and phospholipids (PL) (Gaigg *et al.* 2001; Huang *et al.* 2005; Elle *et al.* 2011) and oxidation (Harris *et al.* 2014). Furthermore, functional loss of ACBP decreases very long-chain FA (VLCFA) content, suggesting that ACBP regulates LCFA elongation and hence VLCFA levels (Gaigg *et al.* 2001; Bloksgaard *et al.* 2012; Neess *et al.* 2013). Finally, ACBP *null* mice have a delayed metabolic adaptation to weaning and impaired epidermal barrier because of altered lipid composition in the skin stratum corneum (Neess *et al.* 2011, 2013; Bloksgaard *et al.* 2012). Collectively, these studies support a key role for ACBP in LCFA-CoA pool formation and metabolism in peripheral tissues.

ACBP is also found throughout the brain with high expression levels in several regions including the hypothalamus (Malagon *et al.* 1993). Interestingly, ACBP is known in neurosciences as diazepam-binding inhibitor (DBI) for its ability to inhibit the binding of diazepam on the benzodiazepine receptor of the $GABA_A$ receptor complex (Guidotti *et al.* 1983). For this reason, ACBP and its proteolytic peptide products, including the octadecaneuropeptide, are termed endozepines.

At the cellular level, ACBP expression has been reported in neurons (Alho *et al.* 1985) and glial cells (Lanfray *et al.* 2013) and its secretion is induced by several stimuli in cultured astrocytes (Tokay *et al.* 2008; Loomis *et al.* 2010). ACBP and its fragments stimulate neurosteroids synthesis (Do Rego *et al.* 2012) and neurogenesis (Alfonso *et al.* 2012) by acting as negative allosteric modulators of the $GABA_A$ receptor. In addition, central administration of octadecaneuropeptide induces anxiety, proconflict behavior (Guidotti *et al.* 1983), and inhibits feeding (Lanfray *et al.* 2013). Together, these studies and others (Christian and Huguenard 2013; Christian *et al.* 2013) suggest that endozepines act as gliotransmitter-modulating neuronal activity by targeting $GABA_A$. Despite this knowledge, whether or not endogenously expressed ACBP regulates LCFA-CoA levels and metabolic fate in the brain and astrocytes remains unknown.

Importantly, astrocytes are known to be the main cell type metabolizing LCFA in the brain (Guzman and Blazquez 2001) and to generate and release unsaturated LCFA (oleate) and polyunsaturated FA (PUFA, arachidonate, and docosahexaenoate) that play important roles in central nervous system function (Moore 2001; Tabernero *et al.* 2001; Camargo *et al.* 2009). In addition, a mounting body of evidence suggests that hypothalamic astrocytes play a key role in the regulation of energy balance by detecting circulating metabolic signals (Chowen *et al.* 2013) including LCFA (Le Foll *et al.* 2014). We recently showed high LCFA oxidative capacity in hypothalamic astrocytes and a glucose-dependent regulation of LCFA oxidation in hypothalamic but not cortical astrocytes (Taib *et al.* 2013). This supports the idea that hypothalamic astrocytes are metabolically equipped to sense nutrients and that ACBP may play a role in LCFA sensing by regulating their metabolism in astrocytes.

Thus, the goal of the present study was to determine whether or not ACBP regulates LCFA metabolism in hypothalamic and non-hypothalamic regions and cultured astrocytes. To this end, we used a combination of cultured astrocytes and hypothalamic slices derived from ACBP-deficient and control mice to measure LCFA-CoA levels, LCFA partitioning between oxidation and esterification as well as FA profile.

Experimental procedures

Reagents

Culture media and serum were from Wisent (Saint-Jean-Baptiste, QC, CA). Radioactive tracers were from PerkinElmer Life Sciences (Waltham, MA, USA) and all other reagents were from Sigma (St Louis, MO, USA) unless otherwise noted.

Animals

ACBP homozygous knockout (KO) mice were kindly donated by Dr Susanne Mandrup (Neess *et al.* 2011) from University of Southern Denmark (Odense, Denmark). Animals were housed two per cage on a 12-h light/dark cycle at 21°C with free access to water and standard chow diet. All procedures were approved by the Institutional Committee for the Protection of Animals (CIPA) at the Centre Hospitalier de l'Université de Montréal. ACBP heterozygous knockout (Het) mice were crossed to generate ACBP wild-type (WT), Het and homozygous knockout (KO) animals. For primary astrocyte cultures, 1- to 2-day-old pups were genotyped from tail clippings. For brain slices and acyl-CoA measurement, mice were genotyped by PCR at weaning as described previously (Bloksgaard *et al.* 2012).

Immunohistochemistry

Male mice were perfused intracardially with 4% formaldehyde under anesthesia. The brains were post-fixed in 4% formaldehyde, cryopreserved in 20% sucrose, and cut into 14 μm serial sections with a cryostat. Sections were blocked and incubated with primary antibodies overnight at 4°C followed by incubation for 1 h at 22°C

with secondary antibodies. Sections were mounted and imaged with a Zeiss fluorescent microscope (Carl Zeiss AG, Jena, Germany). Primary antibodies used were anti-ACBP (1 : 100; kind gift from Dr Mandrup), anti- glial fibrillary acidic protein (GFAP, Mab360, 1 : 100; Millipore Corporation, Bedford, MA, USA) and anti-NeuN (Mab377, 1 : 100; Millipore). Secondary antibodies were Alexa Fluor® 488 Goat Anti-Rabbit IgG and Alexa Fluor® 546 Goat Anti-Mouse IgG (1 : 150; Life Technologies, Carlsbad, CA, USA).

Immunocytochemistry on cultured astrocytes was performed as previously described (Taib *et al.* 2013). Briefly, after fixation in 4% formalin and blocking with 5% bovine serum albumin (BSA) and 0.05% Triton, astrocytes were incubated with the anti-GFAP (1 : 1000) and anti-ACBP (1 : 1000) antibodies in 5% BSA and 0.05% Triton overnight at 4°C followed by secondary antibody incubation (1 : 1000, Alexa Fluor® 568, A-11004; Invitrogen, Carlsbad, CA, USA). The coverslips were mounted onto glass slides with Vectashield (Vector Laboratories, Burlingame, CA, USA) containing 4′,6-diamidino-2-phenylindole DAPI (1.5 μg/mL). Cells were observed with a Zeiss fluorescent microscope. Our cortical and hypothalamic cultures contain ~ 90% of GFAP-positive cells (Taib *et al.* 2013).

Primary astrocyte cultures

Primary cultures of hypothalamic and cortical astrocytes were prepared from 1- to 2-day-old ACBP WT, Het, and KO pups as previously described (Taib *et al.* 2013). Briefly, after decapitation and brain removal, hypothalami and cortices were dissected and mechanically dissociated by passing through syringe needles of decreasing diameter. The cells were plated in poly-L-ornithine-coated six-well plates or T25 and T12.5 flasks and maintained in Dulbecco's modified Eagle's medium (DMEM) containing 25 mm glucose and supplemented with 44 mm $NaHCO_3$, 1% antibiotic-antimycotic, and 10% FBS (Fetal Bovine Serum) at 37°C in 95% O_2, 5% CO_2. Astrocytes were cultured for 14–20 days before use (at ~ 70% confluence).

Western blot analysis

Total protein (25 μg) from ACBP WT, Het, and KO mice was resolved on a 12.5% acrylamide gel and transferred to a polyvinylidene difluoride membrane (Bio-Rad Laboratories, Hercules, CA, USA) blocked with 5% non-fat milk in Tris-buffered saline containing 0.2% Tween 20 for 1 h. Blots were then incubated with an ACBP primary antibody (1 : 1000; Santa Cruz Biotechnology, Santa Cruz, CA, USA) or Actin primary antibody (1 : 200 000) overnight at 4°C followed by secondary antibody incubation horseradish peroxidase-donkey anti-goat (1 : 10 000; Santa Cruz Biotechnology) or goat anti-mouse (1 : 10 000; Bio-Rad) for 2 h at 22°C. Chemiluminescence (Western Lightning, PerkinElmer Life Sciences) was quantified on scanned films using densitometry.

Brain LCFA-CoA levels

LCFA-CoA analysis was performed by HPLC as previously described (Just *et al.* 2006). Hypothalami and cortices were rapidly dissected from ACBP WT and KO fed mice (4–5 weeks old) at the onset of the light cycle and immediately frozen. Heptadecanoyl-CoA (5–8 pmol/mg of tissue) internal standard was added prior to addition of chloroform/methanol (2 : 1). Tissue was then homogenized with an Ultra-turrax homogenizer. Chloroform and H_2O were added and vortexed. After centrifugation, the interphase was recovered and dried under a stream of N_2. The LCFA–CoA were further extracted and derivatized to fluorescent acyl-etheno-CoA esters using 0.5 M chloroacetoaldehyde, 0.5% sodium dodecyl sulfate, 0.15 M citrate, pH 4 (200 μL). Acyl-CoA derivatives were separated and analyzed by reverse phase HPLC (Dionex, Sunnyvale, CA, USA) equipped with a 5-μm LUNA C18 column and a C18 guard column (both from Phenomenex, Torrance, CA, USA) maintained at 40°C. LCFA-CoA were eluted with a constant flow of 0.4 mL/min using solvent A (80% acetonitrile, 20% 20 mM ammoniumacetate) and solvent B (95% 20 mM ammoniumacetate, 5% acetonitrile) with the same gradient as described in (Just *et al.* 2006). Peaks were detected and quantified relatively to the internal heptadecanoyl-CoA standard using the same parameters used in (Just *et al.* 2006). Identification of individual LCFA–CoA was performed using standard LCFA–CoA mixtures derivatized as above-mentioned. The detection level of our methods was 0.5 pmol acyl-CoA/mg protein.

Determination of fatty acid profile in astrocytes

Intracellular free medium-chain fatty acids (MCFA) and LCFA levels as well as MCFA and LCFA released into the incubation media by hypothalamic astrocytes were quantified using HPLC. Hypothalamic astrocytes grown in six-well plates were washed with Krebs-Ringer bicarbonate HEPES (pH 7.4) and cultured during 2 h with Krebs-Ringer bicarbonate HEPES containing 15 mM glucose with 0.5% FA-free BSA or 0.3 mM palmitate complexed to 0.5% FA-free BSA. Cultures were washed with cold phosphate-buffered saline (PBS) prior to MCFA and LCFA extraction. Extraction and HPLC measurements were performed as previously described (Zhao *et al.* 2014). Briefly, FA accumulated in the cells and released into the medium were extracted by Dole–Meinertz extraction procedure (Puttmann *et al.* 1993). The dried FA were derivatized with phenacylbromide and quantified by reverse phase HPLC using a Zorbax Eclipse plus XDB analytical C18 column (4.6.250 mm; 5 μm; Agilent Technology, Santa Clara, CA, USA). FA were eluted using methanol/water (92.5 : 7.5) at a flow rate of 1.5 mL/min and detected at 242 and 254 nm and quantified by the internal standard method. This setup did not allow us to discriminate the signal corresponding to linoleate (C18:2) from docosahexaenoate (C22:6). Results were normalized by cell protein content.

Hypothalamic slices

Hypothalamic slices were generated from ACBP WT and KO mice using modification of a protocol previously used to generate brain slices from rat (Taib *et al.* 2013). Briefly, brains were rapidly removed and immersed in ice-cold cutting solution. Three 300-μm-thick sections containing the hypothalamus were cut from each mouse using a Vibratome (Leica Biosystems, Buffalo Grove, IL, USA) while being continuously immersed and oxygenated in ice-cold cutting solution. The mediobasal hypothalamus (MBH), which includes the arcuate nucleus and the ventro- and dorso-median hypothalamus, was dissected on each section as previously described (Taib *et al.* 2013). MBH slices were allowed to recover for 1 h at 22°C in artificial cerebrospinal fluid (aCSF). Then, slices were pre-incubated at 37°C for 30 min in aCSF containing 1 mM glucose before treatment under constant oxygenation.

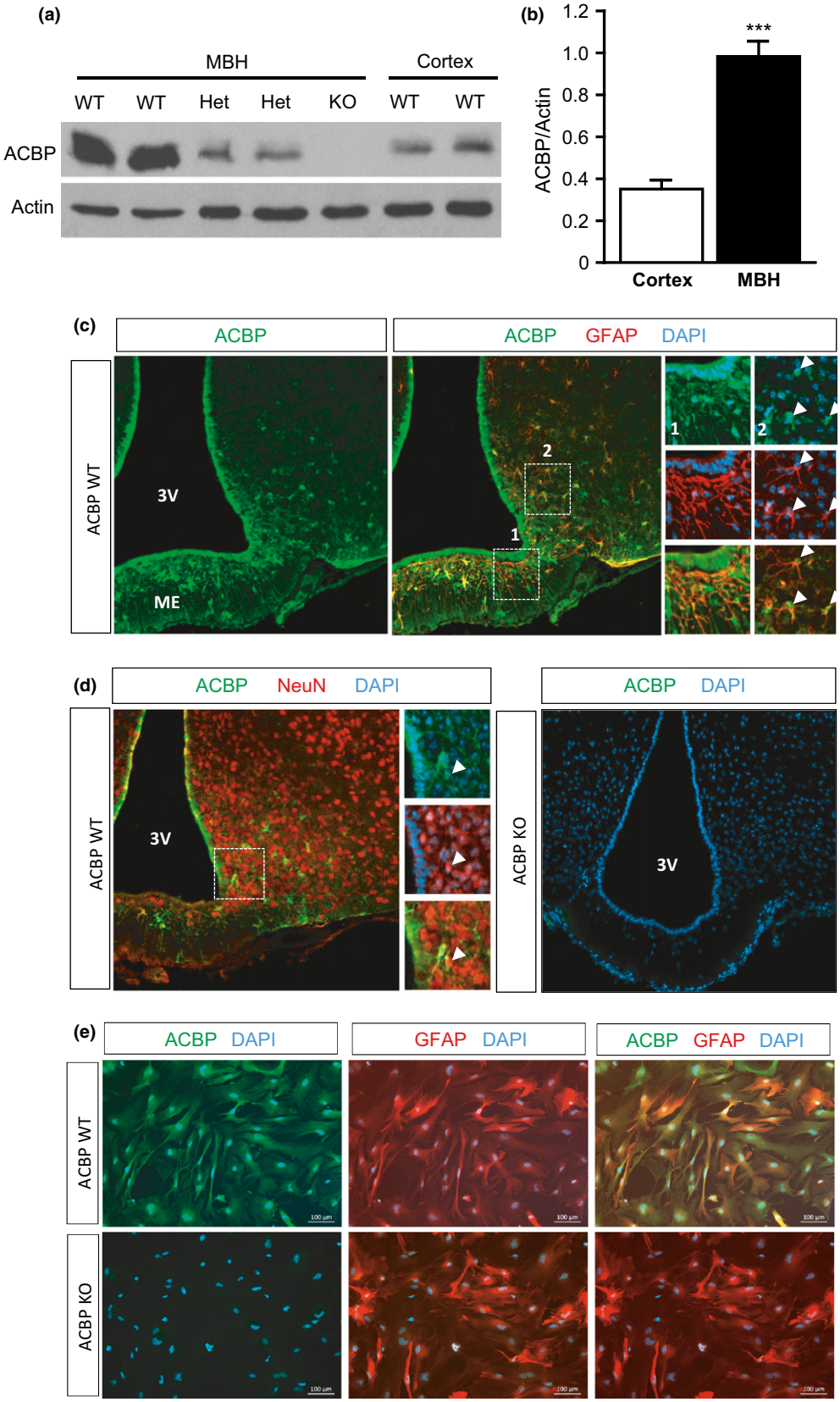
(a)
MBH
Cortex
WT WT Het Het KO WT WT
ACBP
Actin
(b)
ACBP/Actin
1.2
1.0
0.8
0.6
0.4
0.2
0
***
Cortex
MBH
(c)
ACBP
ACBP GFAP DAPI
ACBP WT
3V
ME
1
2
(d)
ACBP NeuN DAPI
ACBP DAPI
ACBP WT
ACBP KO
3V
(e)
ACBP DAPI
GFAP DAPI
ACBP GFAP DAPI
ACBP WT
ACBP KO

Fig. 1 Acyl-CoA binding protein (ACBP) expression in the brain and astrocyte cultures. ACBP expression was determined by western blotting (a) and quantified (b) in the mediobasal hypothalamus (MBH) and cortex of ACBP WT, Het, and KO mice. Co-localization of ACBP immunofluorescence in glial fibrillary acidic protein (GFAP)-(c) and NeuN-positive cells (d) on MBH coronal sections from ACBP WT and KO mice. (e) ACBP and GFAP immunofluorescence in WT (top) and KO (bottom) astrocyte cultures. ME, median eminence; 3V, third ventricle. Results are means ± SEM, $n = 4$, ***$p < 0.001$ (*t*-test).

Oleate transport in astrocytes

Oleate uptake was assessed using radiolabeled oleate. Hypothalamic astrocytes were serum starved during 2 h in DMEM containing 1 mM glucose followed by a 30-min pre-incubation in the same media plus 0.5% FA-free BSA. Cells were then incubated 15 min in presence of 1 mM glucose and 0.3 mM oleate pre-complexed to 0.5% FA-free BSA, 0.2 μCi/mL [1-^{14}C]-oleate, and 0.5 μCi/mL [1-^{3}H(*N*)]-D-manitol. Cells were washed twice with cold PBS and processed for protein extraction and counted to measure [1-^{14}C]-oleate and [1-^{3}H(*N*)]-D-manitol level. Non-specific oleate binding was accounted for by the binding of D-manitol. The results were normalized by cell protein content.

LCFA oxidation in astrocytes and slices

The measurement of LCFA oxidation in primary astrocytes cultures was performed as previously described (Taib *et al.* 2013). Briefly, cells were starved for 2 h in DMEM containing 1 mM glucose followed by a 30-min pre-incubation in the same media plus 0.5% FA-free BSA. Cells were then incubated 2 h in presence of 1 mM glucose and either 0.3 mM palmitate, oleate, α-linolenate, or 0.22 mM stearate pre-complexed to 0.5% FA-free BSA with 0.1 μCi/mL [1-^{14}C]-palmitate, 0.1 μCi/mL [1-^{14}C]-oleate, 0.1 μCi/mL [1-^{14}C]-α-linolenate, or 0.1 μCi/mL [1-^{14}C]-stearate. The incubation was stopped by the injection of 0.2 mL of 40% perchloric acid. After overnight isotopic equilibration at 22°C, $^{14}CO_2$ and ^{14}C acid-soluble products generated by the oxidation of [^{14}C]-palmitate, [^{14}C]-oleate, [1-^{14}C]- α-linolenate, or [1-^{14}C]-stearate were counted to calculate total oxidation. The results were normalized by cell protein content.

Since brain slices have to be constantly oxygenated, ^{14}C-labeled LCFA tracers could not be used to measure LCFA oxidation via the release of $^{14}CO_2$. Therefore, ^{3}H-tracers were employed to estimate the amount of $^{3}H_2O$ generated and released in the media as previously described (Taib *et al.* 2013). Briefly, after pre-incubation in aCSF containing 1 mM glucose and 0.1% BSA for 30 min, MBH slices from ACBP WT and KO mice were incubated during 2 h with 1 mM glucose, 0.1 mM palmitate, or oleate pre-complexed to 0.13% BSA, [9,10(*n*)-^{3}H]-palmitate or [9,10(*n*)-^{3}H]-oleate (2 μCi/mL) at 37°C under constant oxygenation with 95% O_2, 5% CO_2. Incubation media samples were placed in scintillation vials containing cold water and incubated for 24 h at 50°C under constant agitation. After equilibration, $^{3}H_2O$ was counted to calculate palmitate or oleate oxidation. The results were normalized by slice protein content.

LCFA esterification in astrocytes

Oleate and palmitate esterification into neutral lipids was measured using ^{14}C-labeled tracers and thin layer chromatography (TLC) in cultured astrocytes as previously described (Taib *et al.* 2013). Astrocytes grown in T25 flasks were starved for 2 h in DMEM 1 mM glucose followed by a pre-incubation of 30 min in the same media plus 0.5% FA-free BSA. Cells were then incubated during 2 h with 15 mM glucose and 0.3 mM palmitate or oleate pre-complexed to 0.5% FA-free BSA, [1-^{14}C]-palmitate or [1-^{14}C]-oleate (0.1 μCi/mL).

At the end of the incubation, cells were collected, washed with cold PBS, and rapidly frozen in 0.5 mL methanol: HCl (100 : 1) in liquid nitrogen. Total lipids were extracted using the Folch method. Briefly, samples were homogenized using a pestle and loaded into pre-chilled glass tubes containing 2 mL chloroform then washed with 0.5 mL methanol and HCl. Water with 0.9% NaCl was added and samples were vigorously vortexed for 15 s and centrifuged at 900 *g* during 15 min at 4°C. After centrifugation, the lower phase (organic) was transferred into pre-chilled glass tubes and dried under N2. Each sample was suspended in 50 μL chloroform and loaded on the TLC plates (Whatman, Maidstone, Kent, UK). The samples were delivered by small drops and 10 μL of the esterification mix was loaded to quantify total palmitate or oleate tracer radioactivity. Total lipids were separated using a solvent for neutral lipids (petroleum ether/ether/acetic acid; 70 : 30 : 1) for separation of total PL from di- and triacylglycerols (TAG). Plates were imaged using a phosphor screen (GE Healthcare) after 9–10 days exposure and the signal quantified using a Typhoon scanner (GE Healthcare, Little Chalfont, Buckinghamshire, UK). Results were normalized by cell protein content.

Real-time PCR

Real-time PCR was performed as previously described (Taib *et al.* 2013). Briefly, primary astrocytes grown in six-well plates were rinsed with ice-cold PBS before RNA extraction using the TRIzol method (Invitrogen). RNA concentration was quantified spectrophotometrically. About 900 ng of total RNA was reverse-transcribed by M-MuLV reverse transcriptase (Invitrogen) with random hexamers following the manufacturer's conditions. The reaction mix was then diluted fivefold before use. Quantitative gene expression was measured from 1 : 10 cDNA dilutions. Real-time PCR was performed using the QuantiFast SYBR Green PCR kit (Qiagen, Valencia, CA, USA) according to the manufacturer's guidelines on a Corbett Rotor-Gene 6000. Data were analyzed using the standard curve method and normalized to cyclophilin expression levels.

Statistics

Data are expressed as the means ± SEM. Intergroup comparisons were performed by ANOVA analysis with Bonferroni post-tests or by Student's *t*-test when appropriate. $p < 0.05$ was considered significant.

Results

Expression pattern of ACBP

The initial studies of Costa demonstrated that ACBP is expressed in neurons of the rodent brain (Alho *et al.* 1985).

In contrast, recent studies reported either an exclusive expression in glial cells and ependymocytes (Lanfray *et al.* 2013) or expression in both neurons and astrocytes (Christian and Huguenard 2013). We took advantage of the ACBP KO mice to assess the cellular pattern of ACBP expression in the MBH. First, ACBP expression in the MBH is reduced by ~ 50% in ACBP Het and absent in KO mice as expected (Fig. 1a). Second, ACBP protein level is significantly higher in the MBH compared to cortical regions (Fig. 1b). Third, at the cellular level, while ACBP immunofluorescence was observed in scattered neurons of the MBH (NeuN-positive cells, Fig. 1d), most of the signal was detected in GFAP-positive cells in the MBH, median eminence and tanycytes and ependymocytes lining the third ventricle (Fig. 1c). ACBP immunofluorescence was absent in MBH slices from ACBP KO mice (Fig. 1d). In cortical regions, a similar pattern was observed with ACBP expressed in GFAP-positive cells and scattered neurons (data not shown). Finally, in cultured hypothalamic astrocytes, ACBP was detected in ~ 90% of GFAP-positive cells (Fig. 1e). Thus, while ACBP is expressed in few MBH and cortical neurons, its expression is mainly localized in astrocytes and ependymocytes in agreement with previous studies (Christian and Huguenard 2013; Lanfray *et al.* 2013).

ACBP deficiency alters LCFA-CoA profile and unsaturated LCFA metabolism

Given the suggested role of ACBP as a LCFA-CoA pool former (Faergeman *et al.* 2007), we assessed the impact of ACBP deficiency on LCFA-CoA levels in the brain using HPLC. Unlike what was observed in the liver of ACBP KO mice (Neess *et al.* 2011), no general decrease in LCFA-CoA levels was detected in cortical and hypothalamic regions of these mice (Fig. 2a and b). While palmitoyl- (C16) and oleyl-CoA (C18:1) levels were similar in WT and KO brain regions, stearoyl-CoA (C18) level was significantly increased in the cortical and hypothalamic regions of ACBP KO mice.

Since LCFA-CoA levels do not necessarily reflect changes in LCFA metabolic fluxes, we measured oxidation and esterification rates of different type of LCFA, saturated, palmitate (C16), and stearate (C18), as well as unsaturated oleate, (C18:1) and α-linolenate (C18:3), in hypothalamic slices and/or cultured astrocytes. Palmitate, stearate, and

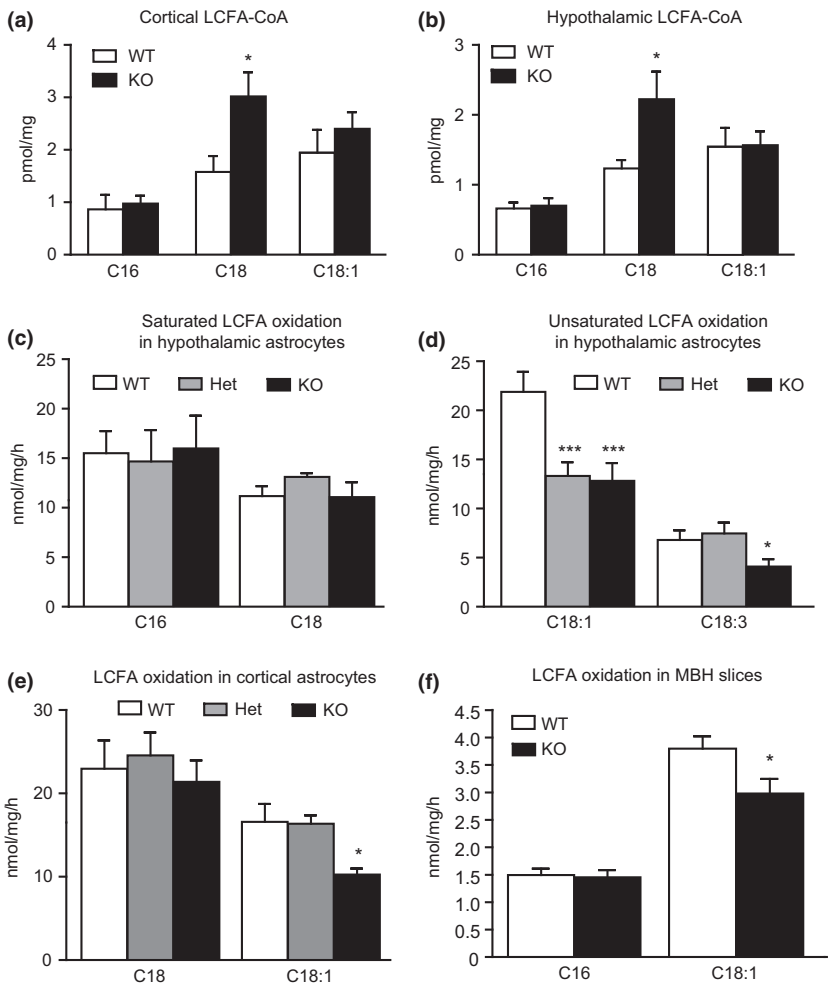

Fig. 2 Acyl-CoA binding protein (ACBP) deficiency alters long-chain fatty acids (LCFA)-CoA levels and impairs oleate oxidation. LCFA-CoA levels in (a) cortex and (b) hypothalamus of WT and KO mice. Palmitate and stearate (c), and oleate and α-linolenate (d) oxidation rates in WT, Het, and KO hypothalamic astrocytes. (e) Stearate and oleate oxidation in WT, Het, and KO cortical astrocytes. (f) Palmitate and oleate oxidation in WT and KO mediobasal hypothalamic (MBH) slices. Results are means ± SEM. $n = 4$–9 for LCFA-CoA levels, $n = 4$–10 for stearate and α-linolenate, $n = 8$–10 for palmitate, and $n = 10$–12 for oleate oxidation. $^{*}p < 0.05$, $^{***}p < 0.001$ (*t*-test and one-way ANOVA).

oleate were chosen because they are the most abundant circulating LCFA (Takahashi *et al.* 2013). In addition, we previously reported a differential metabolic fate of palmitate and oleate in the hypothalamus (Taib *et al.* 2013). Alpha-linolenate is an essential omega-3 PUFA, the precursor of eicosapentaenoate, (20:5) and docosahexaenoate (22:6) synthesis.

In hypothalamic astrocytes derived from ACBP WT, Het, and KO mice, palmitate and stearate oxidation were not affected by the deletion of ACBP (Fig. 2c). In contrast, oleate and α-linolenate oxidation were significantly decreased by ~ 40% in hypothalamic astrocytes (Fig. 2d). A similar pattern was observed in cortical astrocytes in which oleate but not stearate oxidation was decreased by the lack of ACBP (Fig. 2e). To assess whether these results were representative of *in vivo* conditions, oxidation rates were measured in MBH slices derived from 4 to 5 weeks old ACBP WT and KO mice. Similarly to what was observed in astrocytes, oleate but not palmitate oxidation was affected by lack of ACBP in slices (Fig. 2f).

To determine whether alteration of unsaturated LCFA oxidation translates into changes in esterification, we measured the incorporation of oleate and palmitate into neutral lipids including diacylglycerol (DAG), TAG, non-esterified FA, and PL using TLC in MBH slices and astrocyte cultures derived from ACBP WT and KO mice. Oleate was mainly esterified into TAG and PL in astrocytes with higher incorporation into PL in hypothalamic versus cortical astrocytes (Fig. 3a). In cortical astrocytes, oleate esterification was not affected by ACBP deficiency (Fig. 3a) whereas its esterification into TAG and PL was significantly decreased in ACBP KO hypothalamic astrocytes. Importantly, oleate transport was similar in WT and KO hypothalamic astrocytes (3.45 ± 0.7 vs. 3.42 ± 0.4 nmol/mg/h, n = 3–4). In contrast to oleate, palmitate esterification was not affected in MBH slices (data not shown) and hypothalamic astrocytes derived from ACBP KO animals (Fig. 3b). Thus, ACBP deficiency specifically affects unsaturated LCFA metabolism in astrocytes.

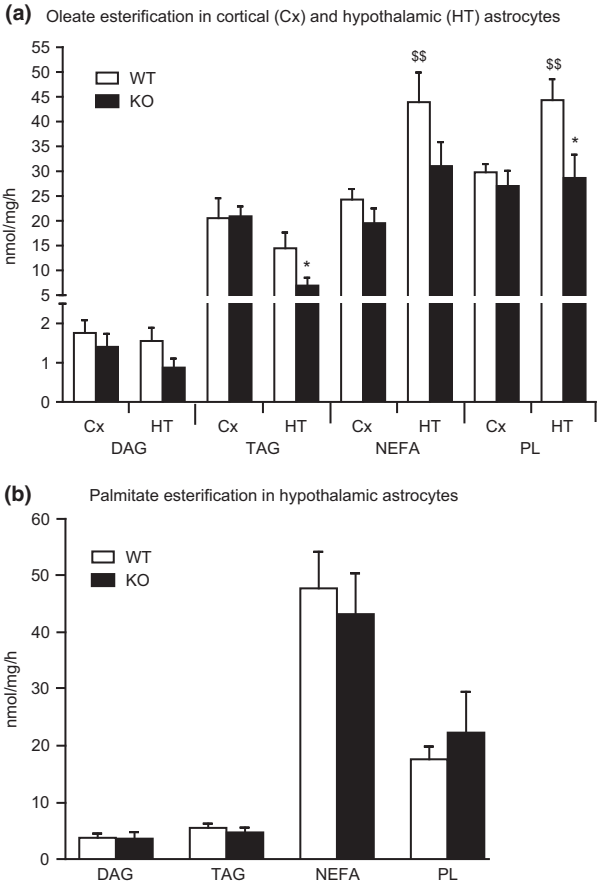

Fig. 3 Acyl-CoA binding protein (ACBP) deficiency alters oleate but not palmitate esterification in hypothalamic astrocytes. (a) Oleate esterification into DAG, triacylglycerol (TAG), non-esterified fatty acid (NEFA), and phospholipids (PL) in astrocytes derived from WT and KO mice and (b) Palmitate esterification in hypothalamic astrocytes. n = 7–10 for oleate esterification and n = 5–10 for palmitate. *p < 0.05 versus WT and $$$p$ < 0.01 versus WT cortical astrocytes (one-way ANOVA).

ACBP deficiency alters the expression of genes involved in LCFA metabolism

We assessed the impact of ACBP deficiency on the expression profile of genes involved in FA transport (cluster of differentiation 36, CD36; fatty acid transport protein 1 and 4), intracellular binding (fatty acid binding protein 7; FABP7), synthesis (acetyl-CoA carboxylase, ACC; fatty acid synthase, FAS), desaturation (stearoyl-CoA desaturase 1), oxidation (carnitine palmitoyl transferase-1a), esterification (glycerol-3-phosphate acyltransferase, GPAT; 1-acylglycerol-3-phosphate acyltransferase, AGPAT; diacylglycerol acyltransferase), and in ceramide synthesis (ceramide synthase, CERS; serine palmitoyltransferase long-chain, SPTLC) in cortical and hypothalamic astrocytes. Only the AGPAT and CERS isoforms showing significant level of expression were studied. FABP7, the predominant FABP isoform in astrocytes (Liu *et al.* 2010), was significantly decreased in cortical and hypothalamic KO astrocytes (Fig. 4a and b). Interestingly, we observed a differential alteration of the gene expression profile in cortical versus hypothalamic astrocytes. In cortical cells, ACBP deficiency led to a decreased expression of genes involved in FA synthesis including ACC1 and FAS, whereas the expression of genes coding for the esterification enzymes AGPAT 1 and 4 was increased in KO astrocytes (Fig. 4a). In hypothalamic astrocytes, the genes mostly affected by ACBP deficiency were those involved in ceramide synthesis, CERS5 and 6, and SPTLC2 (Fig. 4b).

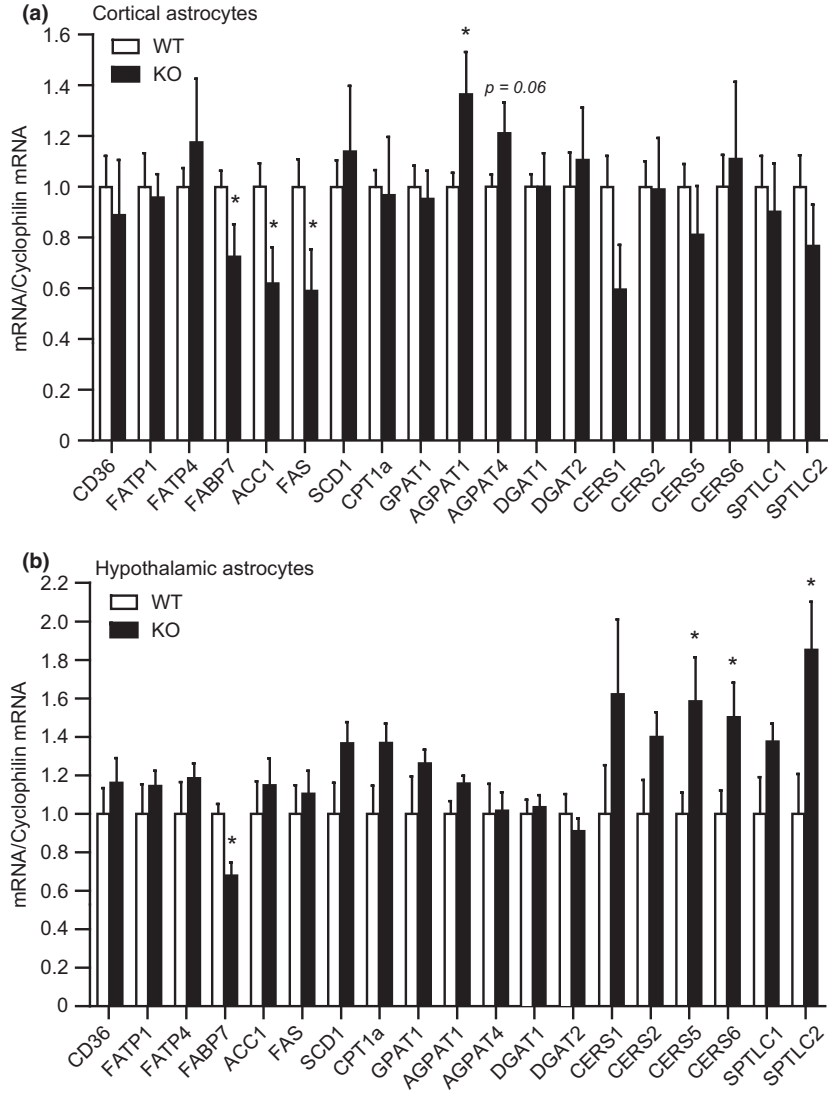

Fig. 4 Acyl-CoA binding protein (ACBP) deficiency alters the expression of genes involved in long-chain fatty acids (LCFA) metabolism. Gene expression was determined by qPCR in WT and KO cortical (a) and hypothalamic (b) astrocytes. mRNA levels were normalized to cyclophilin levels. Results are means ± SEM with $n = 6$–15. $*p < 0.05$ (*t*-test).

The fatty acid profile is altered in ACBP KO hypothalamic astrocytes

To assess more globally the impact of ACBP deficiency on FA profile in astrocytes, we quantified by HPLC the intracellular and extracellular levels of MCFA and LCFA in WT and KO hypothalamic astrocytes in basal and palmitate-treated conditions. Since palmitate partitioning between oxidation and esterification was not affected by lack of ACBP (Figs 2 and 3), we reasoned that palmitate would be a good candidate to test if palmitate desaturation and/or elongation might be affected in ACBP KO cells, and to test the overall impact of palmitate on FA content and release. In WT hypothalamic astrocytes in control conditions, myristate (C14), palmitate (C16), stearate (C18), and oleate (C18:1) were the most abundant intracellular FA (Fig. 5a). Interestingly, the intracellular level of several FA, with the exception of arachidonate (C20:4), was significantly increased in ACBP KO astrocytes (Fig. 5a). The total amount of MCFA and LCFA was significantly increased by ~ 1.4 fold in KO versus WT astrocytes (Fig. 5b). As expected palmitate treatment led to a ~ 1.85 and ~ 1.75 fold increase in intracellular palmitate levels in WT and KO astrocytes, respectively (Fig. 5a). Palmitate significantly increased palmitoleate (C16:1) levels in WT but not KO astrocytes and tended to increase octanoate (C8), myristate and oleate levels in WT astrocytes (Fig. 5a). The total amount of FA was significantly increased in response to palmitate in WT and KO astrocytes with KO cells showing the highest level of FA (Fig. 5b). Thus, ACBP deficiency leads to increased FA levels in astrocytes.

We next investigated whether the capacity of astrocytes to release FA was altered by the lack of ACBP. Octanoate, myristate, palmitate, stearate, and oleate were the most abundant FA found in the media (Fig. 5c). Octanoate level in the media was increased, whereas decanoate (C10), palmitoleate, and arachidonate release was decreased in KO

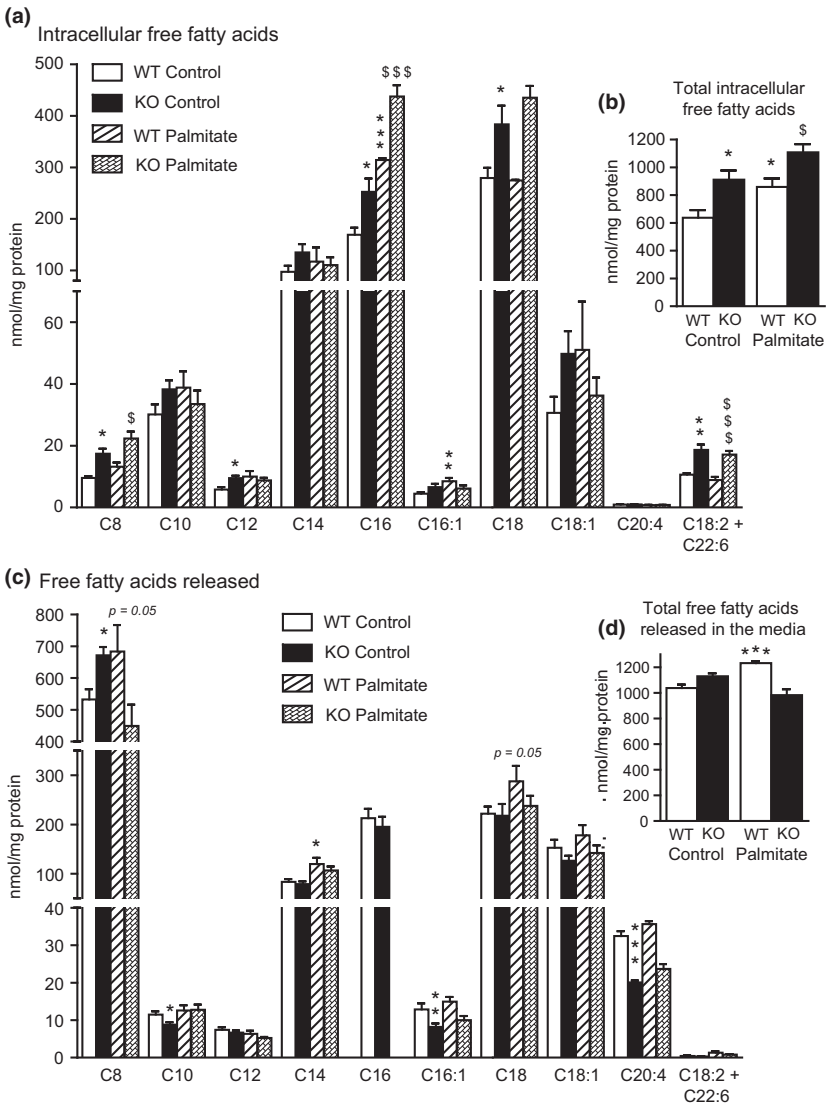

Fig. 5 Modification of the fatty acid (FA) profile in acyl-CoA binding protein (ACBP) KO hypothalamic astrocytes. (a and b) Intracellular content and release (c and d) of different FA species in WT and KO hypothalamic astrocytes treated with or without palmitate (0.3 mM) during 2 h. $n = 6$ to 12 per conditions. *, ** and ***$p < 0.05$, 0.01 and 0.001, respectively, versus WT control. $ and $$$$p < 0.05$ and 0.001, respectively versus WT Palmitate (one- and two-way ANOVA).

astrocytes in control conditions. The total amount of FA released was not significantly affected by ACBP deficiency in basal conditions (Fig. 5d). Palmitate increased media levels of octanoate, myristate, and stearate. The level of palmitate in the media of palmitate-treated cells is not represented in Fig. 5c for scale reasons. The total amount of FA released in the media (without including palmitate) was significantly increased by palmitate in WT but not ACBP KO astrocytes (Fig. 5d). Thus, ACBP deficiency increases intracellular FA levels but decreases FA release from astrocytes.

Discussion

The main objective of this study was to examine the role of ACBP in central LCFA metabolism. Using complementary models derived from ACBP KO mice, we demonstrate that ACBP is mainly expressed in astrocytes *in vivo* and *in vitro* and establish that ACBP deficiency alters LCFA metabolic fluxes (oxidation and esterification) in a LCFA-dependent manner in hypothalamic slice preparations and cultured astrocytes. Furthermore, lack of ACBP differently impacts LCFA esterification and gene expression profile in cortical versus hypothalamic astrocytes. The modifications of LCFA metabolic fluxes in ACBP KO astrocytes were associated with changes in intracellular content and release of different FA species in hypothalamic astrocytes. Taken together, these findings demonstrate for the first time that ACBP is a regulator of LCFA metabolism in astroglial cells.

ACBP has been proposed to act as an acyl-CoA pool former. As a result, the increase in stearoyl-CoA levels observed in the hypothalamus and cortex of ACBP KO mice could seem paradoxical. However, a similar increase has been observed after depletion of ACBP in yeast (Gaigg *et al.* 2001). The reason is unclear but the present observation may have resulted from a central compensatory mechanism and/or changes in circulating LCFA in ACBP KO mice. Plasma FA

levels are similar in 3-week-old WT and KO mice (data not shown), however this does not preclude changes in specific LCFA species. Also, we cannot rule out that other acyl-CoA species or total acyl-CoA level are decreased in ACBP KO brains. Nevertheless, these results show that ACBP deficiency perturbs LCFA-CoA profile in the brain.

Since LCFA-CoA levels do not necessarily reflect changes in LCFA metabolic fluxes, we measured oxidation and esterification rates of different types of LCFA in hypothalamic slices and astrocytes. Our results demonstrate that ACBP deficiency reduces the oxidation of monounsaturated (oleate) and polyunsaturated (α-linolenate) LCFA while saturated LCFA oxidation (palmitate and stearate) is not affected.

The unchanged palmitate and stearate oxidation contrasts with a recent report showing decreased palmitate oxidation in response to ACBP down-regulation in cancer cells (Harris *et al*. 2014). The reason for this discrepancy is unclear but may be explained by differences in the cell type. ACBP has a lower affinity for saturated versus unsaturated LCFA, which is consistent with the specific decrease in oleate and α-linolenate oxidation. In addition, our previous study suggests that oleate oxidation is peroxisomal rather than mitochondrial compared to palmitate in hypothalamic slices (Taib *et al.* 2013). Thus, ACBP might shuttle oleyl-CoA to the peroxisome to undergo oxidation. Alternatively, it is possible that ACBP deficiency in astrocytes interferes with the activity of enoyl-CoA isomerase and dienoyl-CoA reductase, two enzymes required for the oxidation of unsaturated LCFA (Kunau *et al.* 1995).

The notion that ACBP specifically regulates unsaturated LCFA oxidative fluxes was supported by the alteration of oleate but not palmitate esterification into neutral lipids in ACBP KO astrocytes. Interestingly, the decrease in oleate esterification was only observed in hypothalamic astrocytes. Although the reason for this difference between cortical and hypothalamic astrocytes is unclear, the increased expression of the esterification enzymes AGPAT1 and 4 (involved in DAG formation) specifically in cortical astrocytes may contribute to maintaining normal oleate esterification rates in cortical KO cells. Nonetheless, the decreased oleate esterification in ACBP-deficient hypothalamic astrocytes is in agreement with previous studies showing that ACBP down-regulation in *C. elegans* led to a decreased TAG content (Elle *et al.* 2011) while its over-expression increased LCFA esterification into TAG and PL in mouse liver (Huang *et al.* 2005). Importantly, fatty acid transporter expression (CD36 and fatty acid transport proteins) and oleate transport were similar in WT and KO hypothalamic astrocytes, ruling out the possibility that decreased oleate metabolism results from alteration of its uptake.

In line with the idea that loss of ACBP differently impacts cortical versus hypothalamic astrocytes, we found differences in the gene expression profile when comparing cortical and hypothalamic astrocytes lacking ACBP. Indeed, ACBP deficiency resulted in down-regulation of genes coding for enzymes of *de novo* FA synthesis, ACC, and FAS, in cortical astrocytes. This is in agreement with the previous results showing decreased expression of ACC and FAS in the liver of pre-weaned ACBP KO mice (Neess *et al.* 2011). In hypothalamic astrocytes, CERS5 and 6 and SPTLC2 were increased in KO hypothalamic astrocytes suggesting that ACBP might regulate ceramide levels in these cells. Additional studies will be necessary to validate if changes in gene expression translate into changes in FA and/or ceramide synthesis but these findings support the concept that astrocytes from different brain regions have specific FA metabolic features (Taib *et al.* 2013). Of importance, only FABP7 expression was similarly affected by ACBP KO in both cell types. FABP7 is the brain isoform and several lines of evidence support its role in central FA metabolism and action (Liu *et al.* 2010). FABPs are well known to bind FA but are able to bind acyl-CoA as well, though at a much lower affinity compared to ACBP (Knudsen *et al.* 2000). Our gene expression results suggest that ACBP deficiency is not compensated for by increased level of FABP7. On the contrary, lack of ACBP may reduce the overall cellular FA and acyl-CoA binding capacity.

Taken together, our results showing altered expression of endoplasmic reticulum (ER)-associated enzymes (AGPAT, CERS, and SPTLC) and decreased oleate esterification support the role of ACBP in ER function. This is in agreement with the reported localization of ACBP in the ER (Chao *et al.* 2003; Hansen *et al.* 2008). Whether or not ACBP regulates other functions such as ER stress or cholesterol synthesis in astrocytes remains to be determined.

Importantly, our results indicate that intracellular metabolism of unsaturated LCFA is not entirely dependent on ACBP. This is consistent with the expression of other proteins that bind FA and/or acyl-CoA in astrocytes including FABP5 (Liu *et al.* 2010), α-synuclein (Castagnet *et al.* 2005) and Sterol carrier protein-2 (Frolov *et al.* 1996; Micevych *et al.* 2007). Interestingly, the alterations in LCFA metabolic fluxes and FA content observed in KO cells in our study are reminiscent of the changes described in α-synuclein KO astrocytes. Indeed, α-synuclein loss-of-function in cultured astrocytes affects FA uptake, incorporation and distribution in specific lipid pools in a FA-type-dependent manner (Castagnet *et al.* 2005). Similarly, FABP7 loss-of function specifically affects palmitate and arachidonate levels in the brain (Owada *et al.* 2006). Together, these observations suggest that different types and/or isoforms of binding proteins regulate the metabolic fate of specific FA species. Our findings on the FA profile in hypothalamic astrocytes highlight a number of important points.

First, the intracellular content of several LCFA species in astrocytes is in agreement with the levels reported in the brain in which palmitate, stearate, and oleate are the most

represented LCFA (Arsenault *et al.* 2012; Camargo *et al.* 2012). The combined levels of linoleate (C18:2) and docosahexaenoate are relatively low in cultured astrocytes compared to brain levels, which is consistent with the fact that docosahexaenoate is highly enriched in neurons.

Second, ACBP loss-of-function alters the intracellular content of specific MCFA and LCFA in basal conditions leading to an overall increase in the total intracellular FA level. These results are consistent with the reduction in unsaturated LCFA oxidation and esterification rates observed in KO astrocytes (Figs 2 and 3) that may favor FA accumulation. Of interest, FABP7 loss-of-function increases the levels of palmitate and arachidonate in brain lipids (Owada *et al.* 2006). Thus, we cannot rule out that the increased FA content observed in our study results in part from decreased FABP7 expression in ACBP KO cells (Fig. 4). In addition, there is a possibility that ACBP deficiency leads to incomplete unsaturated LCFA oxidation which, in turn, favors the accumulation of MCFA such as octanoate and laurate (Kunau *et al.* 1995). Finally, the increased FA levels found in KO astrocytes may result from decreased LCFA elongation processes. This idea is supported by recent findings showing that lack of ACBP decreases VLCFA content while it increases specific species of LCFA in the skin stratum corneum (Bloksgaard *et al.* 2012).

In terms of palmitate effect on the FA profile, we observed, as expected, that palmitate treatment led to a 1.85-fold increase in intracellular palmitate content in WT astrocytes. The fold increase in palmitate level was similar in KO astrocytes (~ 1.75 fold). We were expecting to detect increased stearate and oleate levels in response to palmitate in WT astrocytes since both LCFA can be generated from palmitate by elongation and elongation plus SCD1-mediated desaturation. Oleate levels tended to be higher in palmitate-treated WT astrocytes but they did not reach statistical significance, making it difficult to determine if oleate content is modulated by palmitate or lack of ACBP. It is conceivable that longer treatment (> 2 h) might be required to modulate stearate and oleate intracellular levels. Interestingly, palmitate-induced accumulation of palmitoleate (monounsaturated palmitate) was impaired in ACBP KO astrocytes, suggesting that ACBP regulates desaturation processes. While the fold increase in total cellular FA content in response to palmitate tended to be lower in KO astrocytes (~ 1.2 vs. ~ 1.35 in WT cells), it was not statistically different compared to WT astrocytes, suggesting that the lack of ACBP does not affect the overall response to exogenous palmitate.

Third, ACBP deficiency alters the release of specific MCFA and LCFA species by astrocytes in basal conditions including octanoate, laurate, palmitoleate, and arachidonate. Of importance, palmitate increased total FA release by ~ 20% in WT astrocytes, a response that was absent in ACBP KO astrocytes, suggesting that ACBP regulates FA release. Although the release of FA species such as myristate and stearate was increased by palmitate, octanoate contributed to most of the overall increase in FA release in response to palmitate in WT astrocytes. It is unclear how lack of ACBP inhibits palmitate-induced FA release. However, the decrease of FABP7 expression in KO astrocytes (Fig. 4) may affect FA cellular trafficking, and therefore their release. To our knowledge, this is the first study reporting the release profile of MCFA and LCFA species in hypothalamic astrocytes and demonstrating that this process is regulated by palmitate in an ACBP-dependent manner. The glial release of oleate and arachidonate is in agreement with previous studies (Tabernero *et al.* 2001; Strokin *et al.* 2003). Our results add to the list of FA released by astrocytes and suggest that they may also provide neurons with myristate, palmitate, and stearate *in vivo*. Octanoate was the most abundant FA found in the media. Whether or not astrocytes release octanoate *in vivo* is unknown. However, it was shown that octanoate can contribute 20% of oxidative metabolism to the brain and constitutes a substrate for glutamine synthesis in astrocytes (Ebert *et al.* 2003), suggesting that astrocyte-derived octanoate may play a significant role as a metabolic substrate *in vivo*.

PUFA including, arachidonate and docosahexaenoate (an essential omega-3 PUFA), are synthesized from omega-3 and -6 precursors and released by astrocytes to regulate important functions in the central nervous system (Moore 2001). The extracellular release of AA and DHA (docosahexaenoate) from membrane PL is regulated by different signals (i.e., ATP and glutamate) in a phospholipase A2-dependent manner in astrocytes (Strokin *et al.* 2003). Interestingly, AA release in ACBP KO astrocytes was significantly decreased in basal conditions. Free cellular arachidonate level was similar in WT and KO astrocytes, however we cannot rule out that arachidonate in membrane PL is decreased in ACBP KO astrocytes. Palmitate did not modulate arachidonate release, suggesting that palmitate does not affect phospholipase A2 activity. In contrast to arachidonate, no changes were observed in the combined media levels of linoleate and docosahexaenoate in response to palmitate or ACBP deficiency. However, since our HPLC analysis did not allow us to discriminate linoleate from docosahexaenoate, we cannot rule out that their respective levels are affected by lack of ACBP. Additional studies using radiolabeled tracers will be required to confirm whether or not ACBP regulates AA and docosahexaenoate release *per se* and if PUFA synthesis from radiolabeled precursors is a process involving ACBP.

One limitation of our study is related to the astrocyte culture model generated from post-natal brain (P1). First, a previous study established that the number of days *in vitro* affects FA composition in cortical astrocytes (Murphy *et al.* 1997). Our astrocyte cultures were used at ~ 70% confluence which was reached after 14–20 days *in vitro*. Thus, it is possible that our results were in part confounded by a variable number of days *in vitro* when comparing different cultures. However, WT, Het, and KO astrocyte cultures were

generated from littermates (ACBP Het breeding scheme) and always used for metabolic measurements after the same number of days in culture, ruling out the possibility that differences observed between WT and KO cells result from the age of the culture. Second, while the adult brain mostly uses glucose as a metabolic substrate, the brain highly relies on ketone bodies and FA during the lactation period (Nehlig 2004). Therefore, it is expected that FA metabolism in cultured P1 astrocytes might be different compared to adult astrocytes. As a result, we cannot rule out that the alterations of LCFA metabolism observed in P1 astrocytes are specific to this developmental stage. However, the fact that a similar decrease in oleate oxidation was observed in hypothalamic slices generated from P30 mice and in P1 astrocytes, suggests that the function of ACBP is conserved and not dependent on the age of the animals.

Altogether, our results show that ACBP deficiency alters the LCFA-CoA profile in the brain, impairs LCFA oxidation and esterification in a LCFA type-dependent manner both in MBH slices and astrocyte cultures, and affects gene expression and FA profile in astrocytes. Our findings suggest that ACBP may play an important role in the hypothalamus. Hypothalamic LCFA action to inhibit feeding and hepatic glucose production mainly relies on their intracellular metabolism (Lam *et al.* 2009). Importantly, the effect of LCFA on feeding is dependent on the type of LCFA. Indeed, unsaturated LCFA, including oleate and docosahexaenoate, but not palmitate, have an anorectic action *in vivo* (Obici *et al.* 2002; Schwinkendorf *et al.* 2010). Our results showing that ACBP specifically affects unsaturated LCFA metabolic fluxes in the hypothalamus, combined with previous studies highlighting the contribution of hypothalamic astrocytes in LCFA metabolism (Taib *et al.* 2013) and sensing (Le Foll *et al.* 2014), make it tempting to speculate that ACBP may be involved in central unsaturated LCFA action on feeding. Further studies using astrocyte-specific ACBP loss-of-function will be required to address this hypothesis.

More generally, our findings suggest that ACBP may regulate central processes and functions known to be modulated by LCFA including neurogenesis, neuroinflammation, and cognition (Haast and Kiliaan 2014).

In summary, our study demonstrates that ACBP, a peptide known so far as an allosteric modulator of the $GABA_A$ receptor in the brain, acts as a regulator of LCFA intracellular metabolism in glial cells. These findings open new research avenues related to its involvement in central nervous system lipid metabolism and functions.

Acknowledgments and conflict of interest disclosure

This project was supported by grants to TA from the Canadian Institutes of Health Research (MOP115042), Fonds de Recherche Quebec-Sante, Societe Francophone du Diabete and Canadian Foundation for Innovation. BT and KB were supported by a doctoral fellowship from Diabete Quebec and University of Montreal. We thank the metabolomics core facility of CRCHUM for their assistance with the measurement of fatty acid profiles. We thank Drs Marc Prentki and Murthy Madiraju for critical discussions.

All experiments were conducted in compliance with the ARRIVE guidelines. The authors have no conflict of interest to declare.

References

Alfonso J., Le Magueresse C., Zuccotti A., Khodosevich K. and Monyer H. (2012) Diazepam binding inhibitor promotes progenitor proliferation in the postnatal SVZ by reducing GABA signaling. *Cell Stem Cell* **10**, 76–87.

Alho H., Costa E., Ferrero P., Fujimoto M., Cosenza-Murphy D. and Guidotti A. (1985) Diazepam-binding inhibitor: a neuropeptide located in selected neuronal populations of rat brain. *Science* **229**, 179–182.

Arsenault D., Julien C., Chen C. T., Bazinet R. P. and Calon F. (2012) Dietary intake of unsaturated fatty acids modulates physiological properties of entorhinal cortex neurons in mice. *J. Neurochem.* **122**, 427–443.

Bloksgaard M., Bek S., Marcher A. B. *et al.* (2012) The acyl-CoA binding protein is required for normal epidermal barrier function in mice. *J. Lipid Res.* **53**, 2162–2174.

Burton M., Rose T. M., Faergeman N. J. and Knudsen J. (2005) Evolution of the acyl-CoA binding protein (ACBP). *Biochem. J.* **392**, 299–307.

Camargo N., Smit A. B. and Verheijen M. H. (2009) SREBPs: SREBP function in glia-neuron interactions. *FEBS J.* **276**, 628–636.

Camargo N., Brouwers J. F., Loos M., Gutmann D. H., Smit A. B. and Verheijen M. H. (2012) High-fat diet ameliorates neurological deficits caused by defective astrocyte lipid metabolism. *FASEB J.* **26**, 4302–4315.

Castagnet P. I., Golovko M. Y., Barcelo-Coblijn G. C., Nussbaum R. L. and Murphy E. J. (2005) Fatty acid incorporation is decreased in astrocytes cultured from alpha-synuclein gene-ablated mice. *J. Neurochem.* **94**, 839–849.

Chao H., Zhou M., McIntosh A., Schroeder F. and Kier A. B. (2003) ACBP and cholesterol differentially alter fatty acyl CoA utilization by microsomal ACAT. *J. Lipid Res.* **44**, 72–83.

Chowen J. A., Argente J. and Horvath T. L. (2013) Uncovering novel roles of nonneuronal cells in body weight homeostasis and obesity. *Endocrinology* **154**, 3001–3007.

Christian C. A. and Huguenard J. R. (2013) Astrocytes potentiate GABAergic transmission in the thalamic reticular nucleus via endozepine signaling. *Proc. Natl Acad. Sci. USA* **110**, 20278–20283.

Christian C. A., Herbert A. G., Holt R. L., Peng K., Sherwood K. D., Pangratz-Fuehrer S., Rudolph U. and Huguenard J. R. (2013) Endogenous positive allosteric modulation of GABA(A) receptors by diazepam binding inhibitor. *Neuron* **78**, 1063–1074.

Do Rego J. L., Seong J. Y., Burel D. *et al.* (2012) Regulation of neurosteroid biosynthesis by neurotransmitters and neuropeptides. *Front. Endocrinol.* **3**, 4.

Ebert D., Haller R. G. and Walton M. E. (2003) Energy contribution of octanoate to intact rat brain metabolism measured by 13C nuclear magnetic resonance spectroscopy. *J. Neurosci.* **23**, 5928–5935.

Elle I. C., Simonsen K. T., Olsen L. C., Birck P. K., Ehmsen S., Tuck S., Le T. T. and Faergeman N. J. (2011) Tissue- and paralogue-specific functions of acyl-CoA-binding proteins in lipid metabolism in Caenorhabditis elegans. *Biochem. J.* **437**, 231–241.

Faergeman N. J., Wadum M., Feddersen S., Burton M., Kragelund B. B. and Knudsen J. (2007) Acyl-CoA binding proteins; structural and functional conservation over 2000 MYA. *Mol. Cell. Biochem.* **299**, 55–65.

Frolov A., Cho T. H., Billheimer J. T. and Schroeder F. (1996) Sterol carrier protein-2, a new fatty acyl coenzyme A-binding protein. *J. Biol. Chem.* **271**, 31878–31884.

Gaigg B., Neergaard T. B., Schneiter R. *et al.* (2001) Depletion of acyl-coenzyme A-binding protein affects sphingolipid synthesis and causes vesicle accumulation and membrane defects in Saccharomyces cerevisiae. *Mol. Biol. Cell* **12**, 1147–1160.

Guidotti A., Forchetti C. M., Corda M. G., Konkel D., Bennett C. D. and Costa E. (1983) Isolation, characterization, and purification to homogeneity of an endogenous polypeptide with agonistic action on benzodiazepine receptors. *Proc. Natl Acad. Sci. USA* **80**, 3531–3535.

Guzman M. and Blazquez C. (2001) Is there an astrocyte-neuron ketone body shuttle? *Trends Endocrinol. Metab.* **12**, 169–173.

Haast R. A. and Kiliaan A. J. (2015) Impact of fatty acids on brain circulation, structure and function. *Prostaglandins Leukot. Essent. Fatty Acids* **92**, 3–14.

Hansen J. S., Faergeman N. J., Kragelund B. B. and Knudsen J. (2008) Acyl-CoA-binding protein (ACBP) localizes to the endoplasmic reticulum and Golgi in a ligand-dependent manner in mammalian cells. *Biochem. J.* **410**, 463–472.

Harris F. T., Rahman S. M., Hassanein M. *et al.* (2014) Acyl-coenzyme A-binding protein regulates Beta-oxidation required for growth and survival of non-small cell lung cancer. *Cancer Prev. Res.* **7**, 748–757.

Huang H., Atshaves B. P., Frolov A., Kier A. B. and Schroeder F. (2005) Acyl-coenzyme A binding protein expression alters liver fatty acyl-coenzyme A metabolism. *Biochemistry* **44**, 10282–10297.

Just M., Faergeman N. J., Knudsen J., Beck-Nielsen H. and Gaster M. (2006) Long-chain Acyl-CoA is not primarily increased in myotubes established from type 2 diabetic subjects. *Biochim. Biophys. Acta* **1762**, 666–672.

Knudsen J., Faergeman N. J., Skott H. *et al.* (1994) Yeast acyl-CoA-binding protein: acyl-CoA-binding affinity and effect on intracellular acyl-CoA pool size. *Biochem. J.* **302**(Pt 2), 479–485.

Knudsen J., Neergaard T. B., Gaigg B., Jensen M. V. and Hansen J. K. (2000) Role of acyl-CoA binding protein in acyl-CoA metabolism and acyl-CoA-mediated cell signaling. *J. Nutr.* **130**, 294S–298S.

Kunau W. H., Dommes V. and Schulz H. (1995) beta-oxidation of fatty acids in mitochondria, peroxisomes, and bacteria: a century of continued progress. *Prog. Lipid Res.* **34**, 267–342.

Lam C. K., Chari M. and Lam T. K. (2009) CNS regulation of glucose homeostasis. *Physiology* **24**, 159–170.

Lanfray D., Arthaud S., Ouellet J. *et al.* (2013) Gliotransmission and brain glucose sensing: critical role of endozepines. *Diabetes* **62**, 801–810.

Le Foll C., Dunn-Meynell A. A., Miziorko H. M. and Levin B. E. (2014) Regulation of hypothalamic neuronal sensing and food intake by ketone bodies and fatty acids. *Diabetes* **63**, 1259–1269.

Liu R. Z., Mita R., Beaulieu M., Gao Z. and Godbout R. (2010) Fatty acid binding proteins in brain development and disease. *Int. J. Dev. Biol.* **54**, 1229–1239.

Loomis W. F., Behrens M. M., Williams M. E. and Anjard C. (2010) Pregnenolone sulfate and cortisol induce secretion of acyl-CoA-binding protein and its conversion into endozepines from astrocytes. *J. Biol. Chem.* **285**, 21359–21365.

Malagon M., Vaudry H., Van Strien F., Pelletier G., Gracia-Navarro F. and Tonon M. C. (1993) Ontogeny of diazepam-binding inhibitor-related peptides (endozepines) in the rat brain. *Neuroscience* **57**, 777–786.

Micevych P. E., Chaban V., Ogi J., Dewing P., Lu J. K. and Sinchak K. (2007) Estradiol stimulates progesterone synthesis in hypothalamic astrocyte cultures. *Endocrinology* **148**, 782–789.

Moore S. A. (2001) Polyunsaturated fatty acid synthesis and release by brain-derived cells in vitro. *J. Mol. Neurosci.* **16**, 195–200; discussion 215-121.

Morton G. J., Cummings D. E., Baskin D. G., Barsh G. S. and Schwartz M. W. (2006) Central nervous system control of food intake and body weight. *Nature* **443**, 289–295.

Murphy E. J., Rosenberger T. A. and Horrocks L. A. (1997) Effects of maturation on the phospholipid and phospholipid fatty acid compositions in primary rat cortical astrocyte cell cultures. *Neurochem. Res.* **22**, 1205–1213.

Neess D., Bloksgaard M., Bek S. *et al.* (2011) Disruption of the acyl-CoA-binding protein gene delays hepatic adaptation to metabolic changes at weaning. *J. Biol. Chem.* **286**, 3460–3472.

Neess D., Bek S., Bloksgaard M., Marcher A. B., Faergeman N. J. and Mandrup S. (2013) Delayed hepatic adaptation to weaning in ACBP-/- mice is caused by disruption of the epidermal barrier. *Cell Rep.* **5**, 1403–1412.

Nehlig A. (2004) Brain uptake and metabolism of ketone bodies in animal models. *Prostaglandins Leukot. Essent. Fatty Acids* **70**, 265–275.

Obici S., Feng Z., Morgan K., Stein D., Karkanias G. and Rossetti L. (2002) Central administration of oleic acid inhibits glucose production and food intake. *Diabetes* **51**, 271–275.

Owada Y., Abdelwahab S. A., Kitanaka N. *et al.* (2006) Altered emotional behavioral responses in mice lacking brain-type fatty acid-binding protein gene. *Eur. J. Neurosci.* **24**, 175–187.

Puttmann M., Krug H., von Ochsenstein E. and Kattermann R. (1993) Fast HPLC determination of serum free fatty acids in the picomole range. *Clin. Chem.* **39**, 825–832.

Rosendal J., Ertbjerg P. and Knudsen J. (1993) Characterization of ligand binding to acyl-CoA-binding protein. *Biochem. J.* **290**(Pt 2), 321–326.

Schwinkendorf D. R., Tsatsos N. G., Gosnell B. A. and Mashek D. G. (2010) Effects of central administration of distinct fatty acids on hypothalamic neuropeptide expression and energy metabolism. *Int. J. Obes. (Lond)* **35**, 336–344.

Strokin M., Sergeeva M. and Reiser G. (2003) Docosahexaenoic acid and arachidonic acid release in rat brain astrocytes is mediated by two separate isoforms of phospholipase A2 and is differently regulated by cyclic AMP and Ca2 + . *Br. J. Pharmacol.* **139**, 1014–1022.

Tabernero A., Lavado E. M., Granda B., Velasco A. and Medina J. M. (2001) Neuronal differentiation is triggered by oleic acid synthesized and released by astrocytes. *J. Neurochem.* **79**, 606–616.

Taib B., Bouyakdan K., Hryhorczuk C., Rodaros D., Fulton S. and Alquier T. (2013) Glucose Regulates Hypothalamic Long-chain Fatty Acid Metabolism via AMP-activated Kinase (AMPK) in Neurons and Astrocytes. *J. Biol. Chem.* **288**, 37216–37229.

Takahashi H., Suzuki H., Suda K. *et al.* (2013) Long-chain free fatty acid profiling analysis by liquid chromatography-mass spectrometry in mouse treated with peroxisome proliferator-activated receptor alpha agonist. *Biosci. Biotechnol. Biochem.* **77**, 2288–2293.

Tokay T., Hachem R., Masmoudi-Kouki O. *et al.* (2008) Beta-amyloid peptide stimulates endozepine release in cultured rat astrocytes through activation of N-formyl peptide receptors. *Glia* **56**, 1380–1389.

Zhao S., Mugabo Y., Iglesias J. *et al.* (2014) Alpha/beta-Hydrolase domain-6-accessible monoacylglycerol controls glucose-stimulated insulin secretion. *Cell Metab.* **19**, 993–1007.